Proceedings of the
44th IEEE Conference on Decision and Control, and
the European Control Conference 2005
Seville, Spain, December 12-15, 2005

Computation of Tight Uncertainty Bounds from Time-domain Data with Application to a Reactive Distillation Column

Marten Völker[1], Sebastian Engell[2]
Process Control Laboratory
Department of Biochemical
and Chemical Engineering
Universität Dortmund
D-44221 Dortmund, Germany
{m.voelker[1],s.engell[2]}@bci.uni-dortmund.de

Abstract— **When deriving data-driven uncertainty descriptions that are compatible with robust controller design methods, it is still a challenge to quantify potentially nonlinear and time-varying model errors. One way to deal with such errors is to choose norm bounds on the error that are not contradicted by measured data which is here called model unfalsification. This methodology enables particularly reliable statements about the model error, if no a priori assumptions about measurement noise are made. Usually, in order to reduce the impact on the control performance, linear filters must be chosen. In this paper, in order to systematise the choice of linear filters, a methodology that minimises the conservatism in the frequency domain while maintaining the unfalsification property in the time domain is proposed, leading to a mixed frequency- and time-domain optimisation problem. The advantages of the approach are that tightness issues can be addressed in the frequency domain while time-domain unfalsification enables the consideration of nonlinearities and time-varying errors. The method is applied to experimental data from a reactive distillation process that exhibits nonlinear and time-varying behaviour.**

I. Introduction

In recent years, the field of optimal linear controller design methods employing frequency-weighted uncertainty descriptions has become very mature [1], [16], [15], [19], [8], [20]. The methodology to ensure robustness by constraining $\mathcal{H}_\infty$ performance channels is a widely accepted tool to design robust control systems. It can be extended to broader classes of systems, such as LPV systems [14]. One way to obtain frequency-dependent bounds that are compatible with the design framework for linear controllers is based upon the analysis of the residuals between model simulation and measured data. In order to generalise this approach, the concept of the model error model, herewith denoted as $\boldsymbol{\Delta}$, is used. The term model error model was mentioned first by [11], although in this context not all possible model representations were addressed: in [11], [9], the model error model is restricted to be of linear FIR (Finite Impulse Response) type similar to [22], where uncertainty descriptions are derived by assuming the residuals to be generated by a stochastic process which entails the assumption that the data was generated by a linear process. We will make use of this concept in an extended fashion comprising possibly nonlinear and time-varying operators which can be considered in the time domain employing a model validation result from [13]. To make sense for robust control, a linear weighting matrix has to be chosen a priori. To the authors' knowledge, no systematic method is available up to now. In this paper, an algorithm is proposed that aims at providing a procedure to find minimal conservative uncertainty weights that are not invalidated (unfalsified) in the sense of [13], where it should be mentioned that the result can be straightforwardly extended to the gain estimation method from [12]. The issue of least conservative uncertainty weights was addressed in the frequency by frequency method from [7], which is, however, restricted to linear model error models. In further contrast, the procedure presented here minimises the conservatism in the frequency domain in a cumulated fashion which offers the possibility to shift error contributions to frequencies where they have smaller impact on the achievable control performance. The paper is organised as follows. After an introduction of notations, a general definition of uncertainty structures is given. Then, techniques for model unfalsification are briefly reviewed. The main part is concerned with the formulation of the optimisation problem to minimise the control-relevant conservatism. Additionally, some numerical issues of the implementation are discussed. Finally, the proposed algorithm is applied to experimental data recorded during closed-loop operation of a reactive distillation column. A linear model is estimated and by means of the new algorithm a multiplicative uncertainty description is derived that is not invalidated by large model errors and and still leads to reasonable performance in robust controller design. For benchmarking, all relevant data can de downloaded via the internet[1].

[1]http://www.bci.uni-dortmund.de
/ast/en/content/mitarbeiter/ewissmitarb/voelker.html

0-7803-9568-9/05/$20.00 ©2005 IEEE

II. Preliminaries

Signals and transfer matrices are considered in discrete-time setting throughout the paper unless otherwise stated. Let $\mathbb{S}^{n_u}$ denote the linear space of all sequences $\{\mathbf{u}(k) \in \mathbb{R}^{n_u}\}_{0 \leq k \leq N-1}$, $1 \leq N \leq \infty$. All linear discrete-time filter operations are denoted by using the shift operator z

$$z^{-1} : \mathbb{S}^{n_u} \rightarrow \mathbb{S}^{n_u} : (\mathbf{u}(0), \ldots,) \rightarrow (0, \mathbf{u}(0), \ldots,),$$

where we do not differentiate between time domain and z-domain as we assume all filter operations $y = W(z) \cdot u$ with zero initial conditions. Multivariate signals and filters are indicated by using bold font. Let

$$l_2^{n_u} = \{\mathbf{u} \in \mathbb{S} : \|\mathbf{u}\|_2^2 = \sum_{k=0}^{\infty} \|\mathbf{u}(k)\|_2^2 < \infty\}$$

denote the Hilbert space of one sided square summable sequences equipped with the usual two-norm that induces the well known l_2-gain or induced 2-norm of a causal operator.

Definition 2.1 (l_2-gain): Let $\mathcal{G}(\bullet) : l_2^{n_u} \rightarrow l_2^{n_y}$ be a possibly nonlinear causal operator so that $\mathbf{y} = \mathcal{G}(\mathbf{u})$. Its l_2-gain γ_2 or its induced 2-norm $\|.\|_{i2}$ is defined as

$$\gamma_2(\mathcal{G}) := \|\mathcal{G}\|_{i2} := \sup_{\mathbf{u} \neq 0} \frac{\|\mathbf{y}\|_2}{\|\mathbf{u}\|_2}.$$

For stable linear systems $\mathbf{W}(z)$, $\gamma_2(\mathbf{W}(z))$ is equal to $\|\mathbf{W}(z)\|_\infty$ equipping the Hardy space $\mathcal{H}_\infty$ of all functions $\mathbf{W}(z)$ that are analytic and bounded outside the unit disc. We also use the well known time truncation operator

$$\pi_k : \mathbb{S}^{n_u} \rightarrow \mathbb{S}^{n_u} : (\mathbf{u}(0), \ldots,) \rightarrow (\mathbf{u}(0), \ldots, \mathbf{u}(k-1)).$$

We use the Matlab-like notation $\mathbf{X}(:, i)$ to denote subparts of matrices; in this case the subpart is the ith column of the matrix $\mathbf{X}$. In the course of the paper, frequent use will be made of the following operators which can be applied to frequency- or time-dependent matrices $(\mathbf{X}(e^{j\omega}), \mathbf{X}(t))$, as well as transfer matrices $(\mathbf{X}(z))$:

- transpose ^{T},
- complex conjugate transpose ^{H},
- stacking operator *col*, where

$$col(\mathbf{X}) := \left[(\mathbf{X}(:,1))^T, (\mathbf{X}(:,2))^T, \ldots, (\mathbf{X}(:,n))^T\right]^T,$$

- *tr* (*trace*), where $tr(\mathbf{X}) := \sum_i X_{ii}$,
- Kronecker operator $\otimes$, where precedence is indicated by using brackets, given by

$$\mathbf{X} \otimes \mathbf{Y} := \begin{bmatrix} X_{11} \cdot \mathbf{Y} & X_{12} \cdot \mathbf{Y} & \ldots & X_{1n} \cdot \mathbf{Y} \\ X_{21} \cdot \mathbf{Y} & \ddots & & \vdots \\ \vdots & & \ddots & \vdots \\ X_{m1} \cdot \mathbf{Y} & & & X_{mn} \cdot \mathbf{Y} \end{bmatrix}.$$

Finally, $\mathbf{I}_m$ denotes the m by m square identity matrix.

III. General model error models

Let a sequence of input values $\mathbf{u} \in l_2^{n_u}$ and of output values $\mathbf{y} \in l_2^{n_y}$ and a potentially nonlinear and time-varying model $\mathcal{G}$ that approximates the mapping $\mathbf{u} \rightarrow \mathbf{y}$ be given. The idea of the model error model is to hypothesise an operator $\mathbf{\Delta}$ that fully explains the input-output data if added to $\mathcal{G}$. The only general assumption on the model $\mathcal{G}$ and the model error model $\mathbf{\Delta}$ is causality. Therefore, the proposed method for the derivation of an uncertainty model is not limited to linear robust control, but can be utilised also in the context of e. g. LPV control with induced norm constraints and linear weighting matrices.

For illustration purposes this concept is depicted for the special case of an output-multiplicative model error model $\mathbf{\Delta}_{om}$ in Fig. 1. The input-output relation of the

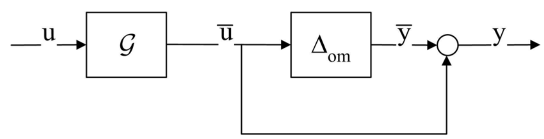

Fig. 1. Example of a model error model.

hypothetical operator $\mathbf{\Delta}$ that is needed for the computation of the model error model from measured data can in most cases (e.g. additive, coprime factor uncertainty) be obtained by filtering. E. g., let

$$\mathbf{y} = \mathcal{G}(\mathbf{u}) + \mathbf{\Delta}_{om}(\mathcal{G}(\mathbf{u})), \tag{1}$$

be the output-multiplicative uncertainty description in Fig. 1, then the input and output sequences of the model error model become

$$\bar{\mathbf{y}} = \mathbf{y} - \mathcal{G}(\mathbf{u}), \quad \bar{\mathbf{u}} = \mathcal{G}(\mathbf{u}),$$

which is easily seen by modifying (1). For the derivation

Uncertainty structure	$\bar{\mathbf{u}}$	$\bar{\mathbf{y}}$
$\mathbf{y} = \mathcal{G}(\mathbf{u}) + \mathbf{\Delta}_a(\mathbf{u})$	$\mathbf{u}$	$\mathbf{y} - \mathcal{G}(\mathbf{u})$
$\mathbf{y} = \mathcal{G}(\mathbf{u}) + \mathbf{\Delta}_{om}(\mathcal{G}(\mathbf{u}))$	$\mathcal{G}(\mathbf{u})$	$\mathbf{y} - \mathcal{G}(\mathbf{u})$
$\mathbf{y} = \mathcal{G}(\mathbf{u} + \mathbf{\Delta}_{im}(\mathbf{u}))$	$\mathbf{u}$	$\mathcal{G}^{-1}(\mathbf{y} - \mathcal{G}(\mathbf{u}))$
$\mathbf{y} = (\mathbf{M} + \mathbf{\Delta}_M)^{-1}(\mathbf{N} + \mathbf{\Delta}_N) \cdot \mathbf{u}$	$[\mathbf{u}^T, -\mathbf{y}^T]^T$	$\mathbf{My} - \mathbf{Nu}$

TABLE I

Model error model input and output sequences for different uncertainty representations.

of our methodology, we use the general model error model input sequence $\bar{\mathbf{u}}$ and output sequence $\bar{\mathbf{y}}$ so that it applies with full generality to all uncertainty descriptions whose inputs and outputs can be obtained by filtering. For clarity, in Tab. I, some filter operations for common uncertainty descriptions are given in an exemplary fashion (from top to bottom: additive, output-multiplicative, input-multiplicative, left-coprime factor uncertainty). It should be noted that the input-multiplicative structure requires invertibility of $\mathcal{G}$ and that the left-coprime factor structure employs the linear model $\mathbf{M}^{-1} \cdot \mathbf{N}$.

IV. Model Unfalsification in the Time Domain

A. General Setup

To derive unfalsified uncertainty bounds from measured data, we consider the following setup. To obtain a less conservative model set for robust control, the model error model mapping $\bar{\mathbf{u}} \to \bar{\mathbf{y}}$ is decomposed as:

$$\bar{\mathbf{y}} = \mathbf{W}_y(z) \cdot \mathbf{\Delta}_c \left(\mathbf{W}_u(z) \cdot \bar{\mathbf{u}} \right), \qquad (2)$$

where $\mathbf{\Delta}_c$ is a potentially nonlinear perturbation with $n_{\tilde{u}}$ inputs and $n_{\bar{y}}$ outputs and $\mathbf{W}_u(z) \in \mathcal{H}_\infty^{n_{\tilde{u}} \times n_{\bar{u}}}$, $\mathbf{W}_y, \mathbf{W}_y^{-1}(z) \in \mathcal{H}_\infty^{n_{\bar{y}} \times n_{\bar{y}}}$ are linear filters; all with zero initial conditions. For the unfalsification of $\mathbf{\Delta}_c$, new variables

$$\tilde{\mathbf{y}} := \mathbf{W}_y^{-1}(z) \cdot \bar{\mathbf{y}}, \quad \tilde{\mathbf{u}} := \mathbf{W}_u(z) \cdot \bar{\mathbf{u}}, \qquad (3)$$

are introduced so that $\mathbf{\Delta_c} : \tilde{\mathbf{u}} \to \tilde{\mathbf{y}}$. The concept is illustrated in Fig. 2. The decomposition (2) can be employed

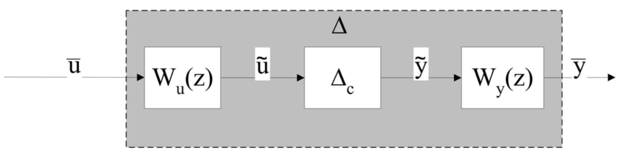

Fig. 2. Internal structure of $\mathbf{\Delta}$

without loss of generality, since the assumptions about a nonlinear operator with neglected internal structure as well as about an operator decomposed as in (2) adhere to the same concept of testing hypotheses.

B. Extension Theorem

For model unfalsification, the extension theorem from [13] is used which assumes that $\mathbf{\Delta}$ be relaxed prior to conducting the experiment. Hence, the data used for unfalsification should be recorded starting close to a steady-state of the true process.

Theorem 4.1 (Operator with bounded l_2-gain): Given the length N input sequence of $\mathbf{\Delta}_c$ $\tilde{\mathbf{u}}^N := \{\tilde{\mathbf{u}}(0), \ldots, \tilde{\mathbf{u}}(N-1) \in \mathbb{R}^{n_{\tilde{u}}}\}$ and the output sequence $\tilde{\mathbf{y}}^N := \{\tilde{\mathbf{y}}(0), \ldots, \tilde{\mathbf{y}}(N-1) \in \mathbb{R}^{n_{\tilde{y}}}\}$, then there exists a stable causal operator $\mathbf{\Delta}_c(\bullet)$ with

$$\|\mathbf{\Delta}_c(\bullet)\|_{i2} \le \gamma, \text{ such that } \tilde{\mathbf{y}}^N = \mathbf{\Delta}_c(\tilde{\mathbf{u}}^N),$$
$$\text{iff} \|\pi_k \tilde{\mathbf{y}}\|_2 \le \gamma \|\pi_k \tilde{\mathbf{u}}\|_2 \quad k = 1, \ldots, N. \qquad (4)$$

Proof: See [13]. ∎

V. Minimum Bounds

A. Problem Specification

A procedure for calculating the tightest uncertainty bounds which are not falsified by the given data is proposed as follows. $\mathbf{W}_y$ is not considered as a degree of freedom in the optimisation and is therefore specified as a fixed invertible minimum phase transfer matrix. Then it can be assumed without loss of generality that $\mathbf{W}_y = \mathbf{I}$, since any invertible weight could be considered by obtaining $\tilde{\mathbf{y}}$ by means of the filter operation $\mathbf{W}_y^{-1} \cdot \bar{\mathbf{y}}$. We formulate the following minimisation problem

$$\min_{\mathbf{W}_u \in \mathcal{H}_\infty, \gamma} \|\gamma \cdot \mathbf{W}_u\|_{Fro}^2 \quad s.t. \quad (4), \qquad (5)$$

with the cumulated Frobenius norm defined by

$$\|\gamma \cdot \mathbf{W}_u\|_{Fro}^2 :=$$
$$\gamma^2 \sum_{i=1}^{N_\omega} tr\left(\mathbf{W}_u^H(e^{j\omega_i}) \cdot \mathbf{W}_u(e^{j\omega_i}) \right) \cdot |l_W(\omega_i)|^2, \qquad (6)$$

where N_ω logarithmically spaced frequency points ω_i are cumulated and l_W is a scalar weighting function. Using the substitution $\mathbf{W}_u = \frac{\mathbf{W}'_u}{\gamma}$ in (4), (5) and the equivalence (3) it is easy to see that the factor γ can be set to any positive real constant without affecting the optimisation objective. Hence, γ vanishes as a degree of freedom of the optimisation (5) and is here set to 1. Unlike a peak-point criterion such as the $\mathcal{H}_\infty$-norm, (5) offers the possibility to tighten the uncertainty in the frequency range in which it has the most limiting impact on the achievable robust control performance. Due to the discretisation of ω_i on a logarithmic grid, high and low frequencies contribute evenly to the optimisation goal (5).

B. Formulation of the Optimisation Problem

We first formulate the problem (5) for $n_{\tilde{u}} = 1$ and then show that, in the case of equal basis functions for each channel, the solution for $n_{\tilde{u}} > 1$ can be derived by a symmetry argument from the $n_{\tilde{u}} = 1$ case. In order to render (5) amenable to a numerical solution the transfer matrix of the filter $\mathbf{W}_u(z) \in \mathcal{H}_\infty^{1 \times n_{\bar{u}}}$ must be represented by a finite series expansion. Here, identical series expansions for each channel are used, given by

$$col(\mathbf{W}_u(z, \mathbf{x})) := \left(\mathbf{I}_{n_{\tilde{u}}} \otimes \mathbf{q}^T(z) \right) \cdot \mathbf{x}, \qquad (7)$$
where $\mathbf{q}^T = [q_0, q_1, \ldots, q_{n_q - 1}] \in \mathcal{H}_\infty^{1 \times n_q}$.

1) Objective function: Employing the finite series expansion (7) and noting that for some complex matrix $\mathbf{A} \in \mathbb{C}^{m \times n}$ it holds that $tr\left(\mathbf{A}^H \cdot \mathbf{A}\right) = (col(\mathbf{A}))^H \cdot col(\mathbf{A})$, the problem (5) can be expressed as

$$\min_{\mathbf{x}} \mathbf{x}^T \cdot \mathbf{H}_{W_u} \cdot \mathbf{x}, \text{ with } \mathbf{H}_{W_u} := \qquad (8)$$
$$\sum_{i=1}^{N_\omega} \Re \left\{ \mathbf{I}_{n_{\tilde{u}}} \otimes \left(\mathbf{q}(e^{-j\omega_i}) \cdot \mathbf{q}^T(e^{j\omega_i}) \right) \cdot |l_W(\omega_i)|^2 \right\},$$

with $\Re\{.\}$ denoting the real part.

2) Constraints: The constraints of the minimisation of (5) are given by the unfalsification conditions (4). With $\gamma = 1$ and squaring both sides of (4), they become

$$\|\pi_k \tilde{\mathbf{y}}\|_2^2 \le \|\pi_k \tilde{u}\|_2^2 \quad k = 1, \ldots, N. \qquad (9)$$

Define the time-dependent variable $\hat{\mathbf{u}}_i := \mathbf{q} \cdot \bar{u}_i$ and the constant data matrix

$$\hat{\mathbf{U}}_{i,k} := \begin{bmatrix} \hat{\mathbf{u}}_i(0) & \hat{\mathbf{u}}_i(1) & \ldots & \hat{\mathbf{u}}_i(k-1) \end{bmatrix}^T. \qquad (10)$$

Then, using (3) and (7), $\pi_k \tilde{u}$ in (9) can be written as

$$\pi_k \tilde{u} = \mathbf{A}_k \cdot \mathbf{x}, \text{ with } \mathbf{A}_k := [\hat{\mathbf{U}}_{1,k}, \hat{\mathbf{U}}_{2,k}, \ldots, \hat{\mathbf{U}}_{n_{\bar{u}},k}].$$

Hence, (9) defines quadratic constraints

$$\mathbf{x}^T \underbrace{(-1) \cdot (\mathbf{A}_k^T \cdot \mathbf{A}_k)}_{:=-\mathbf{P}_k \preceq 0} \cdot \mathbf{x} \leq -\underbrace{\|\pi_k \tilde{\mathbf{y}}\|_2^2}_{:=r_k^2} \quad k = 1, \ldots, N. \tag{11}$$

3) General case ($n_{\tilde{u}} \geq 1$): Let us assume that $\mathbf{W}_u(z)$ has more than one output and is organised in the following block repeated structure:

$$\mathbf{W}_u = \left[col(\mathbf{W}_u(\mathbf{x}_1)) \quad \ldots \quad col(\mathbf{W}_u(\mathbf{x}_{n_{\tilde{u}}})) \right]^T, \tag{12}$$

where each block is given by (7).

Lemma 5.1: We claim that at the optimum of (5) it holds for the block repeated structure (12) that

$$\mathbf{x}_1 = \mathbf{x}_2 = \ldots = \mathbf{x}_{n_{\tilde{u}}}. \tag{13}$$

Proof: Due to (12) it can be inferred that $\|\mathbf{W}_u\|_{Fro}^2 = \sum_{i=1}^{n_{\tilde{u}}} \mathbf{x}_i^T \cdot \mathbf{H}_{W_u} \cdot \mathbf{x}_i$ so that the objective is symmetric with respect to the $\mathbf{x}_i$. Note that, for all k, the constraints $\|\pi_k \tilde{\mathbf{u}}\|_2^2 = \sum_{i=1}^{n_{\tilde{u}}} \|\mathbf{A}_k \cdot \mathbf{x}_i\|_2^2 \geq \|\pi_k \tilde{\mathbf{y}}\|_2^2$ exhibit the same symmetry. Hence, it is concluded that at the optimum of a symmetric objective with symmetric constraints we have $\mathbf{x}_1 = \mathbf{x}_2 = \ldots = \mathbf{x}_{n_{\tilde{u}}}$. ■

Remark 5.1: Due to the equality of rows in the optimal solution it is sufficient to solve (5) for $n_{\tilde{u}} = 1$ reducing the computational complexity.

(11) determines N concave quadratic constraints and therefore yields a nonconvex solution space (see also [3]). Here the problem is solved in two steps, consisting of first solving a convex optimisation problem that is based on replacing the if and only if constraints by one sufficient one and then using the result as a starting point for a gradient-based optimisation in the second step.

C. Approximate Convex Solution

For a single quadratic constraint (N=1) the problem (8) *s.t.* (11) can be solved to optimality by using its dual which can be formulated as a semidefinite program, [3]. This is one of the occasions where a nonconvex optimisation problem can be transferred to a convex optimisation problem and admits no duality gap. Some extensions have been made, see for instance [18], but for more than one nonconvex quadratic constraint, potential dual functions are still an open research item. Hence, to exploit the numerical efficiency of convex optimisation techniques, in this step, we restrict ourselves to a sufficient but not necessary condition for satisfying (11). We proceed as follows. (11) restricts the feasible space to the outside of the ellipsoids $\mathcal{E}_k$ with associated quadratic functions $\mathbf{x}^T \cdot \mathbf{P}_k \cdot \mathbf{x} \leq r_k^2$. Here, the idea is to calculate a minimum volume ellipsoid $\mathcal{E}_0$ with associated quadratic function $\mathbf{x}^T \cdot \mathbf{P}_0 \cdot \mathbf{x} \leq r_0^2$ that fulfils $\mathcal{E}_0 \supseteq \bigcup_{k=1}^{N} \mathcal{E}_k$ using [2], pp. 43, such that a quadratic problem with one nonconvex quadratic constraint

$$\begin{aligned} \mathbf{x}_c := \arg\min \quad & \mathbf{x}^T \cdot \mathbf{H}_{\mathbf{W}_u} \cdot \mathbf{x} \\ s.t. \quad & \mathbf{x}^T \cdot (-\mathbf{P}_0) \cdot \mathbf{x} + r_0^2 \leq 0 \end{aligned} \tag{14}$$

can be solved [3], where $\mathbf{x}_c$ denotes the solution to the convex optimisation problem. Clearly, for the proposed methodology it must be be avoided that, at each k, $\mathbf{P}_k$ has eigenvalues at zero, because this corresponds to ellipsoids of infinite volume. Two causes for such ellipsoids are considered. The first depends on the choice of basis functions, while the second is due to numerical inaccuracies. Counter-measures are introduced for both cases.

1) Choice of Basis Functions: For ease of notation we consider the case where $n_{\bar{u}} = n_{\bar{y}} = 1$ and a single basis q, $n_q = 1 \Rightarrow \mathbf{P}_k = P_k$. The general case follows the same principles. Define the number of trailing zeros at the beginning of the filtered sequence $\hat{u} = q \cdot \bar{u}$ as $d(\hat{u}) := \max_k(\pi_k \hat{u} = \mathbf{0})$, where $\mathbf{0}$ is the zero sequence. Since for $k \leq d(\tilde{y})$ the constraints (11) can be dropped and the corresponding ellipsoids do not need to be considered, the basis function q does not cause a zero eigenvalue of P_k if it is ensured that $d(\hat{u}) \leq d(\tilde{y})$. Define the delay $d(q)$ of the zero initial condition filter $q(z) = \frac{z^m \cdot b_m + \ldots + b_0}{z^n \cdot a_n + \ldots + a_0}$ as the difference between its numerator order and its denominator order $d(q) := n - m$. Therefore, $d(\hat{u}) = d(q) + d(\bar{u})$ so that the final condition for the optimisation bases is

$$d(q) \leq d(\tilde{y}) - d(\bar{u}). \tag{15}$$

Since it is possible to achieve $d(\tilde{y}) = 1$ by scaling and assuming that $d(\bar{u}) = 0$, (15) yields $d(q) \leq 1$. In this paper, generalised Laguerre bases are used that fulfil this property and $d(\bar{u}) = 0$.

2) Regularisation: The problem under investigation is targeted for large scale applications with a couple of thousand ellipsoids. To avoid large condition numbers and numerically caused negative definiteness of $\mathbf{P}_k$, we use $\mathbf{P}_k \leftarrow \mathbf{P}_k + \mathbf{I} \cdot \epsilon$, $\epsilon << \lambda_{max}(\mathbf{P}_k)$, where λ_{max} is the spectral radius and $\leftarrow$ denotes assignment.

D. Nonlinear Optimisation

For the nonlinear optimisation no regularisation is performed. A standard gradient-based solver (Matlab's 'fmincon') inititialised with $\mathbf{x}_c$ is employed to solve the original problem (5). The solution to the nonlinear optimisation is denoted as $\mathbf{x}_n$.

VI. Application Example

A. The Reactive Distillation Column

In this paper, the heterogeneously catalysed esterification of acetic acid and methanol to methyl acetate and water in a pilot plant operated at the Department of Biochemical and Chemical Engineering at Universität Dortmund is studied. The pilot plant is 9 meters high and has a diameter of 100 millimeters. A scheme of the plant is depicted in Fig. 3. It consists of three parts, the reboiler, the condenser and reflux, and the column itself. Within the column, there are three sections of structured packings, two catalytic ones at the bottom and a separating section at the top of the column. Each packing has a length of 1 meter. The plant is operated

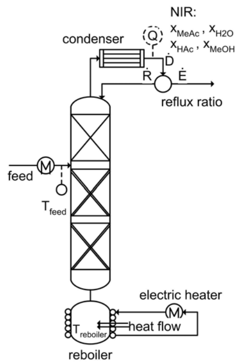

Fig. 3. Scheme of the semibatch reactive distillation column.

in semi-batch mode. This means that, in a first step, the reboiler is filled with methanol which is then evaporated. After the column is filled with methanol vapour, the acetic acid feed is opened and methanol is consumed by the reaction until the concentration of methanol is too low to achieve the desired product concentration. The major degrees of freedom are the reflux ratio[2], the acetic acid feed (feed) and the heat flow supplied to the reboiler via an electrically heated water pipe system. As was shown in [21], the process can be efficiently automated by a robust linear compensator that employs as controlled variables (CVs) the liquid-phase compositions in the reflux $x_{\mathrm{MeAc}}\left[\frac{\mathrm{mole}}{\mathrm{mole}}\right]$ and $x_{\mathrm{H_2O}}\left[\frac{\mathrm{mole}}{\mathrm{mole}}\right]$ which are measured online by near-infrared (NIR) spectroscopy and the reflux ratio and the feed as manipulated variables (MVs). The heat flow is used as an external degree of freedom which is kept at 4 kW using a simple auxiliary control loop. The multivariable controller from [21] was validated in several experiments, one being a setpoint change scenario, designed such that it is possible to estimate a more accurate linear model. Employing a dual Youla parametrisation, [5], of the stabilising controller and the identified model given in [21] and using orthonormal basis functions [6] for the regression aimed at increasing the control relevant accuracy of the identified model. Since the resulting model is of high order and hence of unfavourable numerical tractability, it was reduced via frequency response approximation [4]. The unscaled reduced system (sampling time $T_s = 10$) is given in the appendix in (16). Fig. 4 shows the comparison of reduced-order model simulation (sim) and measured signals (data).

[2]Here defined as the ratio $\frac{\dot{R}}{\dot{D}}$ in the interval $[0, 1]$, see Fig. 3.

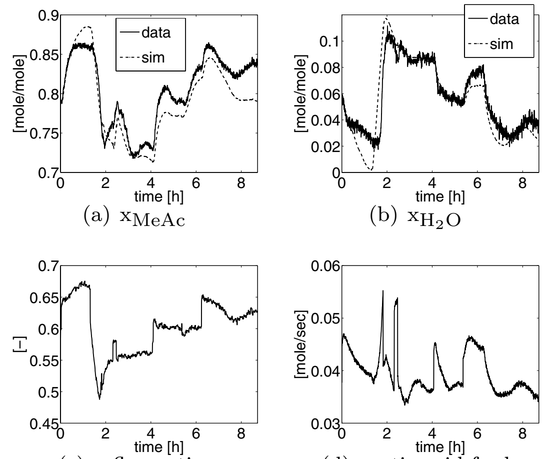

(a) x_{MeAc} (b) $x_{\mathrm{H_2O}}$

(c) reflux ratio (d) acetic acid feed

Fig. 4. Validation data set.

B. Computation of Error Bounds

On the basis of 3140 validation data samples with sampling time $T_s = 10$ seconds, the new procedure was applied to the structure of an output-multiplicative model error model. As basis functions for $\mathbf{q}^T$ generalised Laguerrre transfer functions $q_i(z) = \sqrt{1-a^2}\frac{[-az+1]^i}{[z-a]^{i+1}}\ for\ i = 0\ldots5, a = 0.8$ were used. The objective function was cumulated in the frequency range from 10^{-4} to 10^{-1} at $N_\omega = 200$ frequency points. The weighting function was chosen as $l_W = 10^{-100\cdot\omega}$ entailing the emphasis on low frequencies. All LMI-computations were realised in YALMIP [10] where the Sedumi solver from [17] was interfaced. Let $\mathbf{x}_c$ denote the optimal result from the convex optimisation and let $\mathbf{x}_n$ denote the result from the nonlinear optimisation where $\mathbf{x}_c$ was used as the starting value. Both weighting functions $\mathbf{W}_u(\mathbf{x}_c)$ and $\mathbf{W}_u(\mathbf{x}_n)$ were a posteriori checked by forward evaluation of $\min\gamma\ s.t.$ (4), yielding for the convex result $\gamma_c = 0.91164$ and for the nonlinear optimisation $\gamma_n = 1$. Tab. II shows the values of the objective functions, where the value in brackets corresponds to the multiplication of the convexly optimised value with γ_c^2. The frequency

	Convex opt.	Nonlinear opt.
Objective	25.34 (21.06)	19.63

TABLE II

RESULT OF THE OPTIMISATIONS: OBJECTIVE FUNCTIONS

response of the elements of $\mathbf{W}_u$ is depicted in Fig. 5. It can be seen that a large feasible frequency range for robust control is enabled. Fig. 6 shows the course of the unfalsification constraints $1 - \frac{\|\pi_k\tilde{\mathbf{y}}\|}{\|\pi_k\tilde{u}\|}$ over the experiment time. At approximately 1.9 h it becomes most conservative which coincides with a large transition of MVs and CVs, where the system is operated far outside the range of its nominal operation.

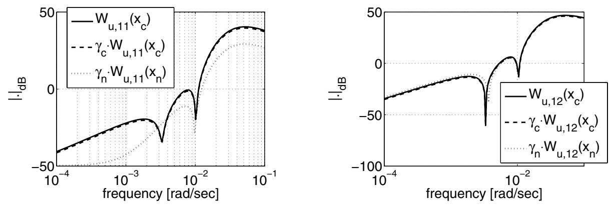

(a) $\mathbf{W}_u(1,1)$ (b) $\mathbf{W}_u(1,2)$

Fig. 5. Minimised model uncertainty bounds.

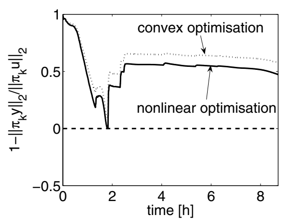

Fig. 6. Unfalsification constraints over time, model is invalidated below the dashed line.

VII. Conclusion

We have shown how to address the issue of model error quantification regarding not only variance errors but also systematic model errors that are caused by nonlinearities and time-varying behaviour. In order to decrease the conservatism of well known model unfalsification results, an optimisation scheme that reduces the control relevant conservatism was proposed and applied to validation data generated by a reactive distillation column with pronounced nonlinear and time-varying characteristics yielding a reasonably large frequency for linear robust control.

VIII. Acknowledgement

Thanks to Johan Löfberg from ETH Zürich for his expertise in ellipsoid approximation, to our colleague Christian Sonntag for supporting the experiments, to Dirk Lieftucht, Queens University Belfast for strengthening our team during technical changes at the plant and to an anonymous reviewer for helpful comments.

Appendix

$$
\begin{aligned}
&G_{11}(s) = \\
&-0.0072\frac{(s-0.1890)(s^2-0.0247s+0.0003)(s+3.64\cdot 10^{-5})}{(s^2+0.0353s+0.0004)(s+0.0007)(s+3.43\cdot 10^{-5})} \\
&G_{12}(s) = \\
&-0.2919\frac{(s-0.0352)(s^2-0.0224s+0.0002)(s+0.0002)}{(s^2+0.0353s+0.0004)(s+0.0007)(s+0.0001)} \\
&G_{21}(s) = \\
&-0.0117\frac{(s+0.1188)(s^2-0.0267s+0.0003)(s+0.0003)}{(s^2+0.0353s+0.0004)(s+0.0015)(s+0.0003)} \\
&G_{22}(s) = \\
&-0.2188\frac{(s-0.0323)(s^2-0.0214s+0.0002)(s+0.0039)}{(s^2+0.0353s+0.0004)(s+0.0071)(s+0.0006)}, \\
&\mathbf{G}(z) = zoh\{\mathbf{G}(s)\}. \qquad (16)
\end{aligned}
$$

References

[1] S. P. Boyd and C. Barrat. *Linear Controller Design: Limits of Performance.* Prentice Hall, Englewood Cliffs, 1991.

[2] S. P. Boyd, L. E. Ghaoui, E. Feron, and V. Balakrishnan. Linear Matrix Inequalities in System and Control Theory. *SIAM*, 1994.

[3] S. P. Boyd and L. Vandenberghe. *Convex Optimization.* Cambridge University Press, 2004. ISBN 0521833787.

[4] S. Engell. Compensator Design by Frequency-Weighted Approximation. *Proceedings of the IEE International Conference on Control*, pages 253–258, 1988.

[5] F. R. Hansen and G. F. Franklin. On a Fractional Representation Approach to Closed-loop Experiment Design. In *Proc. American Control Conference*, pages 1319–1320, Atlanta, USA.

[6] Peter S. C. Heuberger, Paul M. J. Van den Hof, and Okko H. Bosgra. A Generalized Orthonormal Basis for Linear Dynamical Systems. *IEEE Transactions on Automatic Control*, pages 451–465, 1995.

[7] H. Hindi, C. Seong, and S. Boyd. Identification of Tightest Uncertainty Models from Frequency Domain Data. In *Proc. IEEE Conf. on Decision and Control*, 2002.

[8] H. A. Hindi, B. Hassibi, and S. P. Boyd. Multiobjective $\mathcal{H}_2/\mathcal{H}_\infty$-Optimal Control via Finite Dimensional Q-Parametrization and Linear Matrix Inequalities. In *Proc. American Control Conference*, pages 3244–3249, 1998.

[9] R. L. Kosut. Uncertainty Model Unfalsification for Robust Adaptive Control. *Annual Reviews in Control*, pages 65–76, 2001.

[10] J. Löfberg. YALMIP : A Toolbox for Modeling and Optimization in MATLAB. In *Proc. IEEE Conf. on Computer Aided Control Systems Design*, pages 284–289, Taipei, Taiwan, 2004.

[11] L. Ljung. Model Validation and Model Error Modeling. In *Åström Symposium*, number LiTH-ISY-R-2125. Department of Electrical Engineering, Linköping University, March 1999.

[12] L. Ljung. Linear Time-Invariant Models of Non-linear Time-varying Systems. *European Journal of Control*, 2001.

[13] K. Poolla, P. Khargonekar, A. Tikku, J. Krause, and K. Nagpal. A Time-domain Approach to Model Validation. *IEEE Transactions on Automatic Control*, pages 951–959, 1994.

[14] W. J. Rugh and J. S. Shamma. Research on Gain Scheduling. *Automatica*, pages 1401–1425, 2000.

[15] C. W. Scherer. Multiobjective $\mathcal{H}_2/\mathcal{H}_\infty$ Control. *IEEE Transactions on Automatic Control*, pages 1054–1062, 1995.

[16] C. W. Scherer, P. Gahinet, and M. Chilali. Multiobjective Output-Feedback Control via LMI Optimization. *IEEE Transactions on Automatic Control*, pages 896–911, 1997.

[17] J. F. Sturm. Using SeDuMi 1.02, a MATLAB Toolbox for Optimization over Symmetric Cones. *Optimization Methods and Software, Special Issue on Interior Point Methods*, pages 625–653, 1999.

[18] J. F. Sturm and S. Zhang. *On Cones of Nonnegative Quadratic Functions.* Tilburg University, The Chinese University of Hong Kong, 2001.

[19] M. Sznaier, H. Rotstein, J. Bu, and A. Sideris. An Exact Solution to Continuous-time Mixed $\mathcal{H}_2/\mathcal{H}_\infty$ Control Problems. *IEEE Transactions on Automatic Control*, pages 2095–2101, 2000.

[20] M. Völker and S. Engell. Multiobjective Controllability Assessment by Finite Dimensional Approximation. In *Proc. 24th American Control Conference*, pages 39–44, Portland, Oregon, 2005. Paper WeA02.2.

[21] M. Völker, C. Sonntag, and S. Engell. Design of Robust Low-order Controllers for Complex Processes: a Case Study on Reactive Distillation in a Medium-scale Pilot Plant. In *Proc. 16th IFAC World Congress*, Prague, 2005.

[22] Y. C. Zhu. Black-box Identification of MIMO Transfer Functions: Asymptotic Properties of Prediction Error Models. *International Journal of Adaptive Control and Signal Processing*, pages 357–373, 1989.